CrossMark

Exact analysis of heat convection of viscoelastic FENE-P fluids through isothermal slits and tubes

M. Norouzi · S. Z. Daghighi · O. Anwar Bég

Abstract In this article, two exact analytical solutions for heat convection in viscoelastic fluid flow through isothermal tubes and slits are presented for the first time. Herein, a Peterlin type of finitely extensible nonlinear elastic (FENE-P) model is used as the nonlinear constitutive equation for the viscoelastic fluid. Due to the eigenvalue form of the heat transfer equation, the modal analysis technique has been used to determine the physical temperature distributions. The closed form solution for the temperature profile is obtained in terms of a Heun Tri-confluent function for slit flow and then the Frobenius method is used to evaluate the temperature distribution for the tube flow. Based on these solutions, the effects of extensibility parameter and Deborah number on thermal convection in FENE-P fluid flow have been studied in detail. The fractional correlations for reduced Nusselt number in terms of material modulus are also derived. Here, it is shown that by increasing the Deborah number from 0 to 100, the Nusselt number is enhanced by 8.5 and 13.5% for slit and tube flow, respectively.

1 Introduction

Heat convection in straight tubes and channels constitute fundamental and classical problems in the science of heat transfer. The heat convection in Newtonian fluids flowing through closed channels is well established in the literature and significant experimental and theoretical studies have been performed in this regard. However relatively few studies have been communicated concerning heat convection in different types of *non-Newtonian liquids* in either straight tubes or ducts. Heat convection in non-Newtonian liquids is important in diverse areas of modern technology including biotechnology, drug production, pharmaceuticals manufacture (e.g. linctuses), chemical processing industries, food production, cosmetic product synthesis, paint and ink production and injection of polymeric melts (the main method for producing plastics).

Seminal analytical investigations addressing the heat convection in Newtonian fluids in straight channels were presented by Shah [1] and Shah and London [2]. Subsequently considerable theoretical work was conducted in this area and a number of further analytical studies emerged which are reviewed in for example [3, 4]. In the context of non-Newtonian

M. Norouzi (✉) · S. Z. Daghighi
Department of Mechanical Engineering, Shahrood University of Technology, Shahrood, Iran
e-mail: mnorouzi@shahroodut.ac.ir

O. Anwar Bég
Department of Aeronautical and Mechanical Engineering, Salford University, Manchester, UK

flows in conduits and slits, a significant development was made by Oliveira and Pinho [5] and Oliveira [6]. They derived closed-form solutions for internal heat convection in viscoelastic flows through straight pipes and slits using respectively the robust Phan-Thien–Tanner (PTT) and Peterlin finitely extensible nonlinear elastic (FENE-P) fluid models. These studies mobilized a new chapter in rheological heat transfer analysis. Based on the solution of Oliveira and Pinho [5], Coelho et al. [7] have investigated the entrance thermal problem for PTT fluid flow theoretically using the separation of variables technique. They reported that heat transfer characteristics are enhanced by intensifying the shear thinning effect through increasing the parameter εWe^2, where We denotes the Weissenberg number. Pinho and Oliveira [8] studied analytically the problem of fully developed forced convection in pipes and channels with the simplified Phan-Thien–Tanner (SPTT) fluid. Assuming constant wall heat flux and incorporating viscous dissipation, they showed that a combination of elasticity and extensibility increases the Nusselt number. Coelho et al. [9] presented an analytical solution for the fully developed forced convection of PTT fluid in ducts under an imposed constant wall temperature.

Several researchers have also studied *thermally-developing* flow in viscoelastic fluids. Filali et al. [10] have numerically solved the Graetz problem for nonlinear viscoelastic fluids in non-circular tubes deploying the SPTT model. They analyzed the effects of rheological parameters on the heat transfer and validated their results with those findings reported in [7] and [11]. Norouzi [12] presented an analytical solution for heat convection of both linear and exponential PTT fluids in circular pipes with constant wall temperature, describing in detail the effects of Weissenberg number and extensional parameter of the PTT model on heat convection characteristics. Oliveira et al. [12] presented computational solutions for thermally developing FENE-P fluid flow with viscous dissipation in both channel and pipe geometries under constant wall temperature and constant heat flux boundary conditions. Their results revealed that viscous dissipation and elasticity parameter respectively decrease and increase the Nusselt number. Revisiting the analysis of Oliveira et al. [12], Filali and Khezzar [13] simulated the same problem through ducts with various cross sections geometries under

constant wall heat flux without considering viscous dissipation. The results verified the independence of the Nusselt number from the Reynolds number for the FENE-P fluids and also demonstrated agreement with results reported for SPTT fluids by Filali et al. [10]. Iaccarino et al. [14] presented an eddy viscosity model to simulate turbulent flows of homogeneous polymer solutions represented by the FENE-P model. They noted that for both low and high drag reduction conditions, the kinetic energy, polymer elongation profiles and the mean velocity in the channels are in a good agreement with direct numerical simulations (DNS) data. Resende et al. [15] developed a comprehensive low Reynolds number $k - \omega$ model for FENE-P viscoelastic fluids. They validated their work for both low and intermediate drag reductions and reported good correlation of the $k - \omega$ model predictions of the mean velocity with the $k - \varepsilon$ model simulations of Resende et al. [16]. Further, the behavior of the $k - \omega$ model was shown to improve with increasing elasticity in the intermediate drag reduction regime, and additionally performed better with increasing molecular extensibility parameter. Khezzar et al. [17] numerically studied the steady laminar fully developed flow of FENE-P fluid in both circular and non-circular ducts with uniform surface flux neglecting viscous dissipation effects. They computed the Nusselt number distribution and confirmed that the heat transfer rate is enhanced with polymer concentration. Recently Masoudian et al. [18] conducted a DNS study of turbulent heat transfer in channel flow of homogenous polymer solutions modeled by the FENE-P constitutive equation. They developed the first RANS model to predict the heat transfer rates in viscoelastic turbulent flows and computed velocity and mean temperature profiles which were in good agreement with the DNS results. Varagnolo et al. [19] investigated non-Newtonian drops sliding down a planar surface by considering the effects of the polymer solution elasticity. They reported that the drops made of flexible polymers exhibit unusual stretching in a steady sliding, while in the case of stiff polymers the elongation is not observed even at the higher concentrations and this is attributable to interface bending effects enhanced by viscosity. Finally, it is important to mention that flow and heat transfer of the viscoelastic fluids were also studied for annular and non-circular cross sections in both straight [20–24] and curved ducts [25–32].

In present study, the exact analytical solutions for heat convection in FENE-P fluid flow through isothermal tubes and slits are presented for the first time. The slit temperature profile is obtained in terms of the Heun function as a closed form solution. The Frobenius method is used to determine the temperature distribution for the tube flow. The fractional correlations between the reduced Nusselt number and material modulus are also derived. The current analysis strongly indicates that the Frobenius method could be used to find solutions for other complicated isothermal systems and alternate viscoelastic fluid models which would provide a useful benchmark for numerical computations.

2 Governing equations and constitutive equation

The governing equations for internal heat convection of viscoelastic flows comprise the continuity, momentum and energy equations:

$$\nabla . \tilde{\mathbf{V}} = 0 \tag{1a}$$

$$\rho \tilde{\mathbf{V}} . \nabla \tilde{\mathbf{V}} = -\nabla \tilde{p} + \nabla . \tilde{\tau} \tag{1b}$$

$$\rho c_p \tilde{\mathbf{V}} . \nabla \tilde{T} = k \nabla^2 \tilde{T} \tag{1c}$$

where $\tilde{\mathbf{V}}$ is velocity vector, $\tilde{p}$ is pressure, $\tilde{T}$ is temperature, ρ is density, $\tilde{\tau}$ is stress tensor, c_p is specific heat capacity and k is thermal conductivity coefficient. The underlying assumptions for the present study are summarized as follows. The model parameters are independent of temperature, the flow is incompressible, rectilinear, laminar, hydrodynamically and thermally fully-developed, the vicoelastic fluid is simulated with the FENE-P constitutive equation in two dimensions, the velocity profile (along the longitudinal axis) is only dependent on the vertical side and *axial conduction* is negligible relative to *radial conduction*. In light of these assumptions, Eq. (1) can be simplified as follows:

$$\frac{d}{d\tilde{x}}(\tilde{u}(\tilde{y})) = 0 \tag{2a}$$

$$0 = -\frac{d}{d\tilde{x}}\tilde{p}(\tilde{x}) + \frac{1}{\tilde{y}^j}\frac{d}{d\tilde{y}}\left(\tilde{y}^j \tilde{\tau}_{xy}(\tilde{y})\right) \tag{2b}$$

$$\tilde{u}(\tilde{y})\frac{d\tilde{T}(\tilde{y})}{d\tilde{x}} = \alpha \left(\frac{1}{\tilde{y}^j}\frac{d}{d\tilde{y}}\left(\tilde{y}^j \frac{d}{d\tilde{y}}\tilde{T}(\tilde{y})\right)\right) \tag{2c}$$

where α is the thermal diffusivity, $\tilde{y}$ is profile direction (it is identical with $\tilde{y}'$ for the slit scenario and $\tilde{r}$ for the tube case) and j equals 0 for slit flow and 1 for tube flow. Here, the FENE-P model [33] is used as the constitutive equation to determine the stress tensor. The FENE-P equation is derived for dilute solutions but it can be related to semi-dilute solutions which follow the encapsulated dumbbell model from dilute fluids to incompressible Newtonian polymers. The appropriate constitutive equation results from a kinetic theory derivation using a nonlinear elastic dumbbell model [34] to represent the polymer molecules in a dilute solution [35]. In this theory, polymer molecules are modeled as the *dumbbell beads* which are connected to each other via non-Hookean springs. The parameter a is a constant which can be expressed through the extensibility parameters, L and b:

$$a = \frac{1}{1 - 3/L^2} = \frac{b+3}{b}. \tag{3}$$

The FENE-P is one of the rare *molecular constitutive equations* that can be used in computational fluid dynamics and analytical fluid mechanics since it circumvents the need for statistical averaging at each grid point at any instant in time. This equation is able to accurately predict both shear-thinning viscosity and elongational viscosity. The multi-mode form of this model conforms accurately to rheological data of dilute polymeric solutions in oscillation tests. The FENE-P model is also able to predict the polymer turbulence drag reduction. However one drawback of the FENE-P model is that it cannot model the second normal stress difference. According to Bird [37], this constitutive equation arises from a simple molecular theory. However it has furnished a solid platform for understanding of diverse spectrum of rheological phenomena in terms of molecular motion.

3 Formulation

As mentioned before, the principal objective of the current study is to derive, for the first time, exact closed-form solutions for heat convection in FENE-P

fluid flow through tubes and slits. Oliveira [6] presented an exact analytical solution for the velocity field of this problem which takes the form:

$$\frac{\tilde{u}(y)}{U} = \beta_1\left(1 - y^2\right)\left\{1 + \beta_2\left(1 + y^2\right)\right\} \tag{4}$$

where $\tilde{u}$ is the main flow velocity (axial velocity) and U is the mean velocity. In Eq. (4), y is dimensionless profile direction and it is defined as $y = \tilde{r}/\tilde{r}_o$ for tube flow and $y = \tilde{y}'/H$ for slit flow (here, $\tilde{r}$ is the radial direction of tube flow, $\tilde{r}_o$ is the radius of the tube, $\tilde{y}'$ is the lateral direction in slit flow and H is the half distance between the two parallel plates i.e. semi-channel span). The constants β_1 and β_2 can be determined from the following relationships [6]:

For slit flow: $\beta_1 = \dfrac{3}{2}U_N/U, \quad \beta_2 = 9\dfrac{De^2(U_N/U)^2}{a^2L^2},$

$$U_N = -\frac{\tilde{p}_{,\tilde{x}}H^2}{3\eta_0} \tag{5a}$$

For tube flow: $\beta_1 = 2U_N/U, k$

$$\beta_2 = 16\frac{De^2(U_N/U)^2}{a^2L^2}, \quad U_N = -\frac{\tilde{p}_{,\tilde{x}}\tilde{r}_o^2}{8\eta_0}. \tag{5b}$$

In Eq. (5), De is the Deborah number which is defined as $De = \lambda U/H$ for slit flows and $De = \lambda U/\tilde{r}_o$ for tube flows. Oliveira [6] showed that the velocity ratio (U_N/U) can be calculated from the following formulation in terms of rheological properties [6]:

$$\frac{U_N}{U} = \frac{436^{1/6}(\delta^{2/3} - 2^{2/3})}{6\chi^{1/2}\delta^{1/3}} \tag{6}$$

where δ is

$$\delta = (4 + 27\chi)^{1/2} + 3^{3/2}\chi^{1/2}. \tag{7}$$

In Eqs. (6) and (7), χ is a constant which is determined from the following equations [6]:

$$\chi = \frac{54}{5}\frac{De^2}{a^2L^2}\text{(slit)} \quad \& \quad \chi = \frac{64}{3}\frac{De^2}{a^2L^2}\text{(tube)}. \tag{8}$$

The following dimensionless groups are used to normalize the problem i.e. render it non-dimensional:

$$u = \frac{\tilde{u}}{U}, T = \frac{\tilde{T} - \tilde{T}_w}{\tilde{T}_m - \tilde{T}_w} \quad \text{and} \quad Nu = \frac{hd_h}{k}$$

For slit flow: $x = \dfrac{\tilde{x}}{H}, y = \dfrac{\tilde{r}}{H}, \quad \text{and} \quad De = \dfrac{\lambda U}{H}$

For tube flow: $x = \dfrac{\tilde{x}}{\tilde{r}_o}, y = \dfrac{\tilde{r}}{\tilde{r}_o}, \quad \text{and} \quad De = \dfrac{\lambda U}{\tilde{r}_o}$

$$\tag{9}$$

where d_h is the hydraulic diameter (for tube flow: $d_h = 2\tilde{r}_o$ & for slit flow: $d_h = 4H$), $\tilde{T}_m$ is mean temperature, $\tilde{T}_w$ is wall temperature, Nu is the Nusselt number and h is the convective heat transfer coefficient. In the fully-developed thermal condition, the *axial gradient of dimensionless temperature* is zero [4]:

$$T_{,x} = \left(\frac{\tilde{T} - \tilde{T}_w}{\tilde{T}_m - \tilde{T}_w}\right)_{,x} = 0. \tag{10}$$

The following relation is easily derived from the expansion of Eq. (10):

$$\tilde{T}_{,\tilde{x}} = \left(\frac{\tilde{T} - \tilde{T}_w}{\tilde{T}_m - \tilde{T}_w}\right)(\tilde{T}_m)_{,\tilde{x}} = T(\tilde{T}_m)_{,\tilde{x}}. \tag{11}$$

Also, the *axial mean temperature gradient* can be obtained by means of balancing the energy on a differential control volume [4]:

$$h(\tilde{T}_w - \tilde{T}_m)\tilde{P}d\tilde{x} = \rho\tilde{A}Uc_p d\tilde{T}_m$$

$$\Rightarrow \begin{cases} \text{For slit flow: } (\tilde{T}_m)_{,\tilde{x}} = \dfrac{h(\tilde{T}_w - \tilde{T}_m)}{\rho HUc_p} \\[2mm] \text{For tube flow: } (\tilde{T}_m)_{,\tilde{x}} = \dfrac{2h(\tilde{T}_w - \tilde{T}_m)}{\rho\tilde{r}_oUc_p} \end{cases} \tag{12}$$

where $\tilde{P}$ and $\tilde{A}$ denote the perimeter and area of the conduit cross-section, respectively. Regarding Eqs. (2c), (9), (11) and (12), the non-dimensional form of the heat transfer equation for the FENE-P fluid flow can be expressed as follows:

$$T_{,yy} + \frac{j}{y}T_{,y} + \frac{1}{4 - 3j}Nu.\beta_1\left(1 - y^2\right) \times \left[1 + \beta_2\left(1 + y^2\right)\right]T = 0 \tag{13}$$

where j = 0 and j = 1 correspond to the slit and tube cases, respectively. The boundary conditions for this equation consist of a constant wall temperature and a symmetry condition at the centerline. Also, the finite value of temperature at the centerline (no singularity

point in temperature field) can be used as the boundary condition for only the tube flow case, which is suitable for eliminating the singular solution from the final solution of this problem.

$$at \; y = 0 \Rightarrow T_{,y}$$
$$= 0 \; (\text{or finite/nonsingular solution for tube flow}) \quad (14a)$$

$$at \; y = 1 \Rightarrow T = 0. \quad (14b)$$

The boundary value problem defining fully developed isothermal internal heat convection, which is introduced in Eq. (13) is an *eigenvalue differential equation* since both differential equations and boundary conditions are *homogeneous* and an *unknown constant* (Nu) exists in the equation. Therefore unlike in other problems of heat convection, it is necessary to determine a Nusselt number that satisfies the governing equation and boundary conditions and finally obtain the temperature distribution (Note- the procedure for obtaining the solution is inverse for other problems where firstly the temperature distribution is calculated and secondly the Nusselt number is determined from the temperature field). In this paper, the possible value of the Nusselt number is obtained by *modal analysis* of Eq. (13) under the boundary condition introduced in Eq. (14). Due to the homogenous form of the governing equation and boundary conditions, they are not sufficient to obtain the non-zero temperature distribution and a *non-homogenous* condition or a *non-homogeneous* constraint is required to complete the solution. Here, a constraint is presented by integrating the product of dimensionless velocity profile ($u = \tilde{u}/U$) into the dimensionless temperature distribution ($T = (\tilde{T} - \tilde{T}_w)/(\tilde{T}_m - \tilde{T}_w)$) for the entire cross section. The solution of this integration can be easily calculated as follows:

$$\int\limits_0^1 y^j u(y) T(y) dy = \frac{1}{1+j}. \quad (15)$$

Using the above constraint, the coefficients of the solution of Eq. (13) will be calculated and the temperature distribution will be obtained.

4 Analytical solution of heat convection

4.1 Slit flow

The solution of heat convection of FENE-P fluid flow in a slit is obtained by solving Eq. (13) and considering $j = 0$. The solution of this second order differential equation can be expressed as follows:

$$T(y) = C_1 F_1(y) + C_2 F_2(y) \quad (16)$$

where

$$F_1(y) = e^{\frac{1}{12} \frac{Nu \beta_1 y (2 y^2 \beta_2 + 3)}{\sqrt{Nu \beta_1 \beta_2}}} HeunT \left(0.13 \frac{Nu^2 \beta_1^2 (2 \beta_2 + 1)^2}{(Nu \beta_1 \beta_2)^{4/3}}, \right.$$
$$\left. 0, 0.72 \frac{Nu \beta_1}{(Nu \beta_1 \beta_2)^{2/3}}, -0.69 \sqrt[6]{Nu \beta_1 \beta_2} y \right) \quad (17a)$$

$$F_2(y) = e^{-\frac{1}{6} \frac{Nu \beta_1 y (y^2 \beta_2 + 3/2)}{\sqrt{Nu \beta_1 \beta_2}}} HeunT \left(0.13 \frac{Nu^2 \beta_1^2 (2 \beta_2 + 1)^2}{(Nu \beta_1 \beta_2)^{4/3}}, \right.$$
$$\left. 0, 0.72 \frac{Nu \beta_1}{(Nu \beta_1 \beta_2)^{2/3}}, 0.69 \sqrt[6]{Nu \beta_1 \beta_2} y \right) \quad (17b)$$

where *HeunT* is the Heun Tri-confluent function. A summary about introducing the hypergeometric function is provided for readers in Appendix A. In order to obtain the Nusselt number, we should use the boundary conditions defined in Eq. (14).

$$at \; y = 0 \rightarrow T_y = 0 : C_1 F_1'(0) + C_2 F_2'(0) = 0 \quad (18a)$$

$$at \; y = 1 \rightarrow T = 0 : C_1 F_1(1) + C_2 F_2(1) = 0. \quad (18b)$$

The above set of equations is homogenous and therefore its solution will be *non-zero* if it is linearly dependent (determinant of Eq. (18) should be equal to zero):

$$\begin{vmatrix} F_1'(0) & F_2'(0) \\ F_1(1) & F_2(1) \end{vmatrix} = 0. \quad (19)$$

The remaining unknown of Eq. (19) is the Nusselt number and also Eq. (19) can be expanded as follows:

For any Deborah number and extensibility parameter (L), it is possible to determine the constants of velocity profile (β_1 and β_2) from Eq. (5). Therefore,

$$G(Nu) = -\frac{\sqrt{Nu\beta_1}}{4\sqrt{\beta_2}} \left(\begin{array}{l} HeunT\left(0.13\,\dfrac{Nu^2\beta_1^2(2\beta_2+1)^2}{(Nu\beta_1\beta_2)^{4/3}}, 0, 0.72\,\dfrac{Nu\beta_1}{(Nu\beta_1\beta_2)^{2/3}}, -0.69\,\sqrt[6]{Nu\beta_1\beta_2}\right) \mathrm{e}^{1/12\frac{Nu\beta_1(2\beta_2+3)}{\sqrt{Nu\beta_1\beta_2}}} + \\[3mm] \mathrm{e}^{-1/12\frac{Nu\beta_1(2\beta_2+3)}{\sqrt{Nu\beta_1\beta_2}}}\,HeunT\left(0.13\,\dfrac{Nu^2\beta_1^2(2\beta_2+1)^2}{(Nu\beta_1\beta_2)^{4/3}}, 0, 0.72\,\dfrac{Nu\beta_1}{(Nu\beta_1\beta_2)^{2/3}}, 0.69\,\sqrt[6]{Nu\beta_1\beta_2}\right) \end{array} \right).$$

$$\tag{20}$$

for known values of β_1 and β_2, the Nusselt number can be obtained by calculating the roots of $G(Nu)$ (This function is defined in Eq. (20)). For example, the graph of $G(Nu)$ versus Nu is plotted in Fig. 1 at $De =$
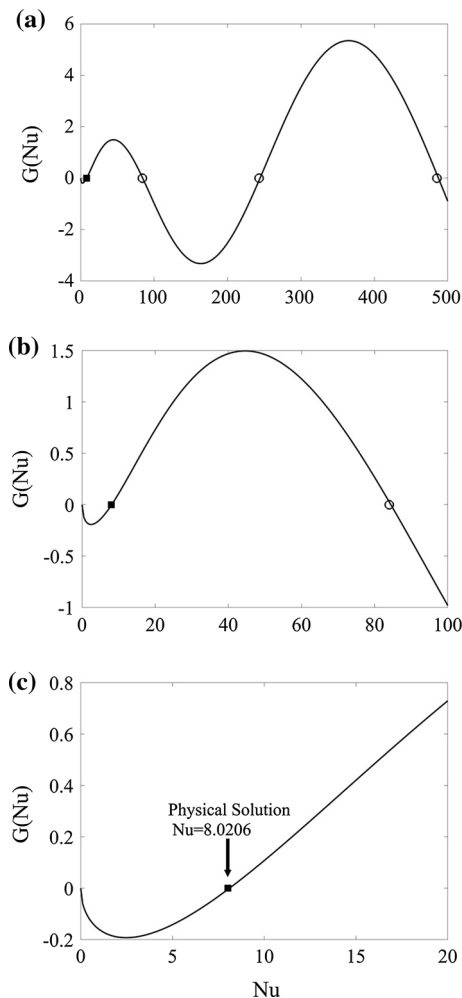
Fig. 1 Diagrams of $G(Nu)$ versus Nusselt number for an isothermal slit at $L^2 = 10$ and $De = 10$

10 and $L^2 = 10$. For clearer display we present the distribution of $G(Nu)$ in three different ranges of Nu. According to Fig. 1, this function has infinite discrete roots. According to the scaling law, the Nusselt number in laminar closed channels is of first order. This root is specified by a filled square in Fig. 1 and denotes that $Nu = 8.0206$.

After determining the Nusselt number, we should find the remaining constants of C_1 and C_2 to complete the solution of heat convection of FENE-P fluid flow in a slit. Owing to a linear dependence between Eq. (18a) and (18b), we should use one of them to determine the constants. The other non-homogenous equation which is necessary for extracting C_1 and C_2 can be obtained by substituting Eqs. (4) and (16) into the Eq. (15) and performing the resulting integration. In this case (case of Fig. 1), $C_1 = 0.6788$ and $C_2 = 0.6792$.

4.2 Tube flow

The solution of heat convection of FENE-P fluid flow inside a circular tube can be obtained by solving Eq. (13) by substituting $j = 1$. Unfortunately, there is no closed form solution for this problem based on the known mathematical functions. For this reason, the Frobenius method is used to find the Taylor series expansion of this problem.

Generally, any second order differential equation can be specified in the following general form:

$$P(x)f'' + Q(x)f' + R(x)f = 0 \tag{21}$$

where P, Q, and R are the arbitrary polynomials. The roots of $P(x)$ are the singularity points provided that at least one of the other polynomials ($Q(x)$ and $R(x)$) is non-zero at these roots. Assuming that x_0 is a singularity point, this is designated as a regular

singular point provided the following conditions are satisfied [38]:

$$\lim_{x \to x_0} (x - x_0) \frac{Q(x)}{P(x)} \text{ is finite} \tag{22a}$$

$$\lim_{x \to x_0} (x - x_0)^2 \frac{R(x)}{P(x)} \text{ is finite.} \tag{22b}$$

Based on the conditions presented in Eq. (22), it is evident that the center of the tube ($y = 0$) is a regular singular point of Eq. (13). Therefore, the tube temperature distribution for FENE-P fluid flow can be derived by applying the Frobenius method on Eq. (13) with $j = 1$, as follows:

thermal boundary condition at the wall. By applying the boundary condition presented in Eq. (14b) on the temperature distribution, a polynomial in terms of Nu is obtained. In Appendix B, this polynomial is presented up to seventh order (refer to Eq. (34)). According to the scaling law in heat convection, the Nusselt number in internal laminar flow is of the first order. Therefore, the first order positive root of Eq. (34) is the physical Nusselt number of the FENE-P fluid flow. It is evident that C_1 is equal to the maximum value of dimensionless temperature since the maximum dimensionless temperature is located at the center of the tube ($r = 0$). Therefore, the temperature distribution of FENE-P fluid flow

$$
T(y) = C_1 \left(
\begin{array}{l}
1 - \dfrac{1}{2} \dfrac{Nu}{a^2 L^2} (\dfrac{U_N}{U})^3 \left((\dfrac{U}{U_N})^2 a^2 L^2 + 16 De^2 \right) y^2 + \\[2em]
\dfrac{1}{32} \dfrac{Nu}{a^4 L^4} (\dfrac{U_N}{U})^6 \left(\begin{array}{l} \left(2 Nu + 4 \dfrac{U}{U_N} \right) (\dfrac{U}{U_N})^4 a^4 L^4 + \\[1em] 64 Nu De^2 (\dfrac{U}{U_N})^2 a^2 L^2 + 512 Nu De^4 \end{array} \right) y^4 + O(y^6)
\end{array}
\right)
$$

$$
+ \, C_2 \left(
\begin{array}{l}
\ln(y) \left(
\begin{array}{l}
1 - \dfrac{1}{2} \dfrac{Nu}{a^2 L^2} (\dfrac{U_N}{U})^3 \left((\dfrac{U}{U_N})^2 a^2 L^2 + 16 De^2 \right) y^2 + \\[2em]
\dfrac{1}{32} \dfrac{Nu}{a^4 L^4} (\dfrac{U_N}{U})^6 \left(\begin{array}{l} \left(2Nu + 4 \dfrac{U}{U_N} \right) (\dfrac{U}{U_N})^4 a^4 L^4 + \\[1em] 64 Nu De^2 (\dfrac{U}{U_N})^2 a^2 L^2 + 512 Nu De^4 \end{array} \right) y^4 + O(y^6)
\end{array}
\right) \\[5em]
+ \dfrac{1}{2} \dfrac{Nu}{a^2 L^2} (\dfrac{U_N}{U})^3 \left((\dfrac{U}{U_N})^2 a^2 L^2 + 16 De^2 \right) y^2 \\[2em]
+ \left(\dfrac{1}{8} Nu \dfrac{U_N}{U} - \dfrac{3}{64} \dfrac{Nu}{a^4 L^4} (\dfrac{U_N}{U})^6 \left(\begin{array}{l} \left(2Nu + 4 \dfrac{U}{U_N} \right) (\dfrac{U}{U_N})^4 a^4 L^4 + \\[1em] 64 Nu De^2 (\dfrac{U}{U_N})^2 a^2 L^2 + 512 Nu De^4 \end{array} \right) \right) y^4 + O(y^6)
\end{array}
\right)
\tag{23}
$$

It is important to remember that the temperature distribution is *finite* over the whole of the cross section. Therefore, based on the Eq. (14a), the term C_2 should be zero to remove the singular solution at $r = 0$. The Nusselt number can be calculated using the

inside the isothermal tube, can be presented with greater accuracy as Eq. (24).

After calculating the Nusselt number from Eq. (34), the remaining constant of temperature distributions (C_1) can be determined by substitution of Eqs. (4) and

(24) into the constraint presented in Eq. (15) and by taking $j = 1$ into account.

In Appendix B, the formulation of this constant (T_{max}) is presented (refer to Eq. (35)).

5 Results and discussion

5.1 Verification

The present analytical solution is verified in two ways: firstly via comparing the results with the analytical solution for the Newtonian case and secondly by comparison with numerical solutions for FENE-P fluid flow. The FENE-P constitutive equation is reduced to the Newtonian model by considering $De = 0$. In this

$$
\frac{T(y)}{T_{\max}} = \left(
\begin{array}{l}
1 - \dfrac{1}{2}\dfrac{Nu}{a^2 L^2}\left(\dfrac{U_N}{U}\right)^3\left(\left(\dfrac{U}{U_N}\right)^2 a^2 L^2 + 16\,De^2\right)y^2 \\[2mm]
+ \dfrac{1}{32}\dfrac{Nu}{a^4 L^4}\left(\dfrac{U_N}{U}\right)^6\left(
\begin{array}{l}
\left(2\,Nu + 4\dfrac{U}{U_N}\right)\left(\dfrac{U}{U_N}\right)^4 a^4 L^4 + 64\,Nu\,De^2\left(\dfrac{U}{U_N}\right)^2 a^2 L^2 + \\[2mm]
512\,Nu\,De^4
\end{array}
\right)y^4 \\[4mm]
- \dfrac{1}{288}\dfrac{Nu}{a^6 L^6}\left(\dfrac{U_N}{U}\right)^9\left(
\begin{array}{l}
\left(Nu^2 + 10\,Nu\dfrac{U}{U_N}\right)\left(\dfrac{U}{U_N}\right)^6 a^6 L^6 + \\[2mm]
\left(48\,Nu^2 De^2 + 160\,Nu\,De^2\dfrac{U}{U_N} - 256\,De^2\left(\dfrac{U}{U_N}\right)^2\right)\left(\dfrac{U}{U_N}\right)^4 a^4 L^4 + \\[2mm]
768\,Nu^2 De^4\left(\dfrac{U}{U_N}\right)^2 a^2 L^2 + 4096\,Nu^2 De^6
\end{array}
\right)y^6 \\[6mm]
+ \dfrac{1}{36864}\dfrac{Nu^2}{a^8 L^8}\left(\dfrac{U_N}{U}\right)^{12}\left(
\begin{array}{l}
\left(4\,Nu^2 + 112\,Nu\dfrac{U}{U_N} + 144\left(\dfrac{U}{U_N}\right)^2\right)\left(\dfrac{U}{U_N}\right)^8 a^8 L^8 + \\[2mm]
\left(256\,Nu^2 De^2 + 3584\,Nu\,De^2\dfrac{U}{U_N} - 10240\,De^2\left(\dfrac{U}{U_N}\right)^2\right)\left(\dfrac{U}{U_N}\right)^6 a^6 L^6 + \\[2mm]
\left(
\begin{array}{l}
6144\,Nu^2 De^4 + 28672\,Nu\,De^4\dfrac{U}{U_N} - \\[2mm]
163840\,De^4\left(\dfrac{U}{U_N}\right)^2
\end{array}
\right)\left(\dfrac{U}{U_N}\right)^4 a^4 L^4 + \\[2mm]
65536\,Nu^2 De^6\left(\dfrac{U}{U_N}\right)^2 a^2 L^2 + 262144\,Nu^2 De^8
\end{array}
\right)y^8
\end{array}
\right) + \ldots
$$

$$(24)$$

condition, the Nusselt number for the present study in an isothermal slit flow (Eqs. (16) to (20)) is equal to 7.541 which is exactly equal to the Nusselt number reported in the literature (see for example Bejan [39]). The Nusselt number of Newtonian fluid flow in the isothermal tube is reported as around 3.66 in the literature [4, 39] which is obtained using successive approximations. Recently, Norouzi and Davoodi [40] obtained an exact closed form analytical solution for this problem as follows:

$$T = \frac{1.09615}{r} M_{0.6761,0}\left(2.7044r^2\right) \tag{25}$$

where M is the mth-kind of Whittaker function. Based on this solution, the Nusselt number and dimensionless temperature at the center of the tube are $Nu_0 = 3.6568$ and $T_{\mathbf{max,0}} = 1.8026$ [40]. It is important to remember that the solution of heat convection of FENE-P fluid flow in isothermal tubes is obtained using Frobenius method. By calculating up to the eighth order terms in the Frobenius series (Eq. (24)) and considering $De = 0$, we have $Nu = 3.6571$ and $T_{max} = 1.8025$ which shows good agreement with the results reported by Norouzi and Davoodi [40].

We have further verified the analytical solutions for heat convection in FENE-P fluid flow by comparing
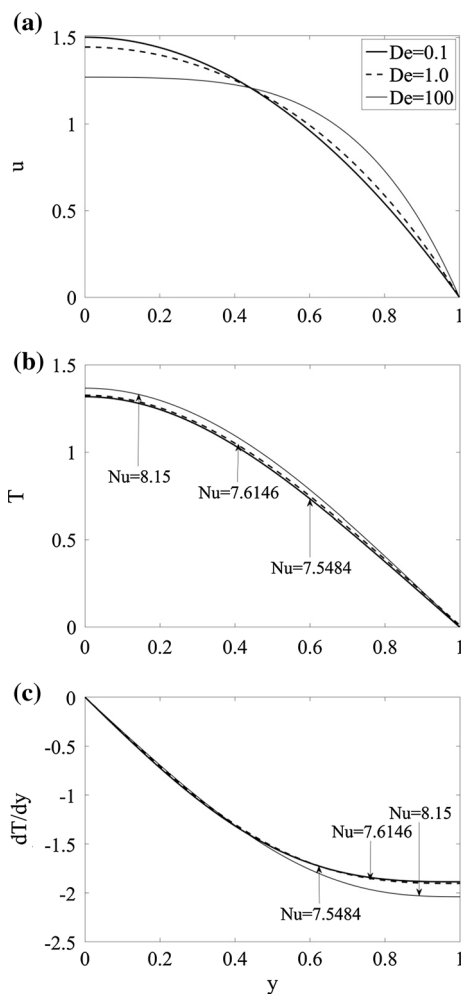
Fig. 2 Profiles of velocity and temperature of FENE-P fluid in an isothermal slit at $L^2 = 10$ for different values of Deborah number. a axial velocity, b temperature and c lateral temperature gradient
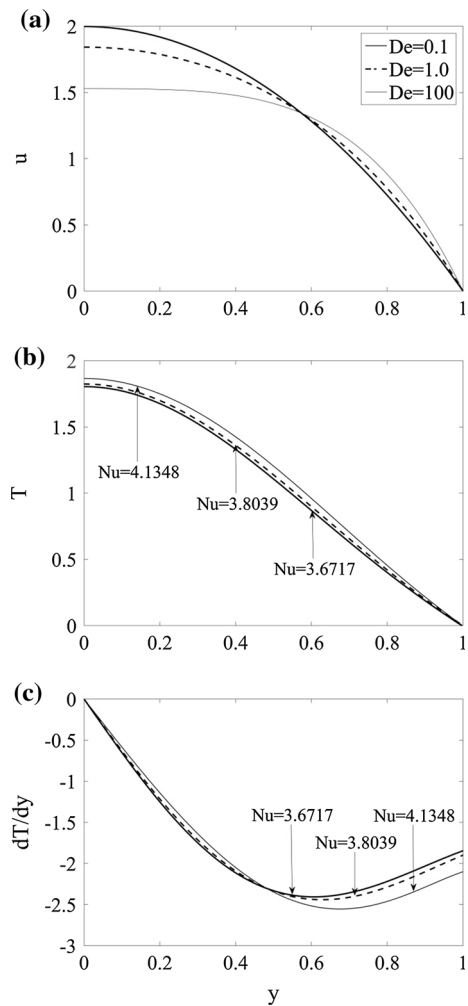
Fig. 3 Profiles of velocity and temperature of FENE-P fluid in an isothermal tube at $L^2 = 10$ for different values of Deborah number. a axial velocity, b temperature and c radial temperature gradient

Table 1 Nusselt number data for FENE-P fluid flow in an isothermal slit for different Deborah numbers at three values of extensibility parameter

De	Nu	C_1	C_2	β_1	β_2
$L^2 = 10$					
0.1	7.5484	0.6586	0.6586	1.4945	0.0044
1	7.6146	0.6617	0.6706	1.1478	0.2582
10	8.0206	0.6788	0.6792	0.3647	2.6072
20	8.0787	0.6813	0.6810	0.2380	4.4406
30	8.1036	0.6832	0.6806	0.1842	5.9829
40	8.1180	0.6825	0.6829	0.1532	7.3608
50	8.1275	0.6834	0.6825	0.1327	8.6278
60	8.1345	0.6811	0.6858	0.1179	9.8128
70	8.1396	0.6837	0.6832	0.1067	10.9336
80	8.1438	0.6817	0.6859	0.0978	12.0022
90	8.1471	0.6859	0.6813	0.0906	13.0271
100	8.1500	0.6906	0.6763	0.0846	14.0148
$L^2 = 100$					
0.1	7.5447	0.0060	− 0.1043	1.5008	0.0008
1	7.5782	0.6607	0.6606	1.3832	0.0720
10	7.9202	0.6749	0.6751	0.5878	1.3004
20	7.9507	0.6595	0.6997	0.3947	2.3455
30	8.0463	0.6797	0.6802	0.3088	3.2304
40	8.0693	0.6813	0.6801	0.2585	4.0227
50	8.0848	0.6807	0.6823	0.2247	4.7520
60	8.0961	0.6825	0.6809	0.2003	5.4344
70	8.1048	0.6830	0.6811	0.1816	6.0801
80	8.1118	0.6814	0.6838	0.1667	6.6959
90	8.1173	0.6824	0.6829	0.1546	7.2866
100	8.1220	0.6840	0.6813	0.1445	7.8560

Table 2 Nusselt number data for FENE-P fluid flow in an isothermal tube for different Deborah numbers at three values of extensibility parameter

De	Nu	T_{max}	β_1	β_2
$L^2 = 10$				
0.1	3.6717	1.8048	1.9828	0.0077
1	3.8039	1.8244	1.3550	0.3598
10	4.0517	1.8574	0.3952	3.0609
20	4.0896	1.8616	0.2559	5.1355
30	4.1056	1.8633	0.1975	6.8788
40	4.1148	1.8643	0.1640	8.4357
50	4.1209	1.8649	0.1419	9.8670
60	4.1248	1.8652	0.1260	11.2056
70	4.1286	1.8657	0.1140	12.4716
80	4.1308	1.8658	0.1044	13.6785
90	4.1329	1.8660	0.0967	14.8361
100	4.1348	1.8663	0.0902	15.9516
$L^2 = 100$				
0.1	3.6628	1.8034	1.9991	0.0015
1	3.7147	1.8109	1.7397	0.1139
10	3.9851	1.8496	0.6472	1.5762
20	4.0429	1.8564	0.4285	2.7643
30	4.0686	1.8593	0.3335	3.7666
40	4.0834	1.8609	0.2783	4.6630
50	4.0936	1.8620	0.2415	5.4876
60	4.1008	1.8628	0.2149	6.2589
70	4.1064	1.8634	0.1947	6.9887
80	4.1108	1.8639	0.1786	7.6845
90	4.1144	1.8642	0.1655	8.3519
100	4.1174	1.8645	0.1546	8.9951

the results with numerical solutions. The solution of Eq. (13) can be obtained using second order finite difference discretization. In the case of tube flow, we can cancel the singularity situation by avoiding the term $T_{,y}/y$ at the center of the tube (applying the boundary condition (14a)). At last, the discretized form of Eq. (13) for isothermal slits and tubes can be specified as follows:
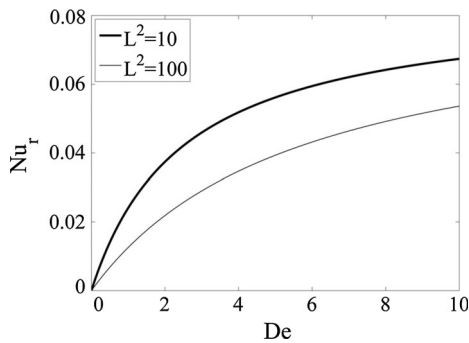
$$A_{ij}T_j = NuT_j \Rightarrow (A_{ij} - Nu\delta_{ij})T_j = 0 \qquad (26)$$

where A_{ij} is the tri-diagonal matrix of coefficients of discretization and δ_{ij} is the Kronecker delta. According to the Eq. (26) and scaling law, the Nusselt number is the first order eigenvalue of A_{ij}. Due to the symmetric form of A_{ij}, the eigenvalues are obtained

using the Jacoby method [41]. Here, the Nusselt number is computed using 500 grid points and the convergence condition of Jacoby method is enforced by decreasing the value of non-diagonal elements of the mapped matrix of A_{ij} to less than 10^{-6}. The maximum deviation of the present analytical solution for slit and tube flow from the numerical solution is less than 1.7% at $L^2 < 100$ and $De < 10$. This small deviation could be attributed to the truncation error of numerical solution and also the truncation of Frobenius series.

Table 3 Nusselt number data and constants of temperature profile for slit and tube flow in terms of De/aL
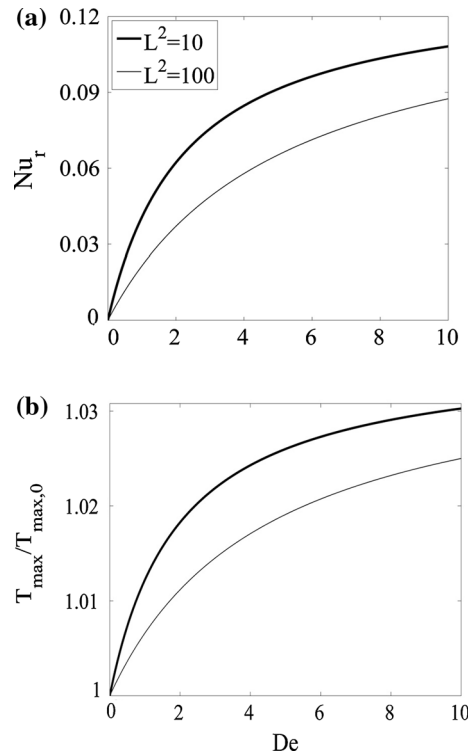
De/aL	Slit			Tube	
	Nu	C_1	C_2	Nu	T_{max}
0.1	7.6278	0.6615	0.6582	3.7138	1.8104
0.2	7.6613	0.6643	0.6643	3.7923	1.8229
0.3	7.7891	0.6714	0.6601	3.8450	1.8307
0.4	7.8378	0.6748	0.6609	3.8824	1.8359
0.5	7.8756	0.6776	0.6613	3.9121	1.8402
0.6	7.8809	0.6767	0.6658	3.9280	1.8419
0.7	7.8861	0.6754	0.6699	3.9439	1.8436
0.8	7.8914	0.6738	0.6738	3.9598	1.8453
0.9	7.9091	0.6745	0.6747	3.9777	1.8487
1.0	7.9833	0.6868	0.6612	3.9863	1.8494
2.0	8.0102	0.6785	0.6786	4.0449	1.8566
3.0	8.0488	0.6800	0.6800	4.0703	1.8595
4.0	8.0718	0.6810	0.6807	4.0850	1.8611
5.0	8.0848	0.6810	0.6817	4.0935	1.8620
6.0	8.0979	0.6808	0.6833	4.1020	1.8629
7.0	8.1334	0.6810	0.6817	4.1067	1.8634
8.0	8.1690	0.7325	0.6301	4.1113	1.8638
9.0	8.1740	0.7364	0.6267	4.1147	1.8642
10.0	8.1790	0.7431	0.6199	4.1182	1.8646

Fig. 5 Diagrams of (**a**) reduced Nusselt number and (**b**) ratio of the maximum temperature of FENE-P fluid flow to the Newtonian one versus Deborah number for different values of L^2

Fig. 4 Diagram of reduced Nusselt number in an isothermal slit versus Deborah number for different values of L^2

5.2 Effect of rheological properties on heat convection

In this section, the effects of rheological properties characterizing the FENE-P model (extensibility parameter and Deborah number) on heat convection in slit and tube flow are studied. Figures 2 and 3 illustrate the velocity and temperature profiles in

isothermal slit and tube scenarios, respectively. These diagrams are plotted at $L^2 = 10$ for different values of Deborah number. It is evident from the plots that increasing Deborah number tends to increase the flatness of the velocity profile and decrease the maximum value of axial velocity. It is also apparent that the velocity gradient is increased near to the wall. This can be attributed to an intensification in the shear-thinning behavior of FENE-P fluid which manifests in a reduction in fluid viscosity in the vicinity of the wall, associated with higher Deborah number. The present solutions are corroborated with similar reports in the literature [5, 6, 12, 42] which also describe an accentuation in bluntness of velocity profile connected with stronger shear-thinning behavior of non-Newtonian liquids at greater Deborah number. According to Figs. 2 and 3, the temperature and Nusselt number are increased with a rise in Deborah number. This effect is induced by elevating the velocity gradient near to the wall. The data of Nusselt number, constants of temperature formulation (Eq. (16)) and constants of

a velocity profile for *slit flow* (Eq. (4)) are presented in Table 1. These data are obtained for $0 < De \leq 100$ and $L^2 = 10$ and 100 which cover a wide range of realistic rheological properties of viscoelastic liquids. The corresponding results for *tube flow* are documented in Table 2. It is important to remember that the temperature distribution of FENE-P fluid flow is obtained using the Frobenius method and a constant ($T_{\max}$) is utilized in the execution of this solution (see Eq. (24)). The maximum temperature for different values of Deborah number is reported in Table 3. According to Tables 2 and 3, by increasing the Deborah number from 0 to 100, the Nusselt number is boosted up to 8.5 and 13.5% for the slit and tube flow cases, respectively.

The reduced Nusselt number is a useful dimensionless group which denotes the difference between the heat convection of non-Newtonian and Newtonian flows:

$$Nu_r = \frac{Nu - Nu_0}{Nu_0}. \tag{27}$$

Here Nu_0 is the Nusselt number of the Newtonian flow and it is equal to 7.5410 and 3.6568 for isothermal slit and tube, respectively. The evolution of reduced Nusselt number with variation in Deborah number for the slit and tube flow scenarios, respectively, are illustrated in Figs. 4 and 5. The distribution of maximum temperature for tube flow is also depicted in Fig. 5b. According to these plots, the reduced Nusselt number and $T_{\max}$ are enhanced asymptotically by increasing the Deborah number and decreasing the extensibility parameter. This indicates that a fractional correlation exists between the reduced Nusselt number and rheological properties. It is important to remember that the constants of velocity distribution (β_1 and β_2) are dependent on De/aL for both slit and tube flow (see Eqs. (4) to (8)). Consequently, the temperature distribution and Nusselt number should likewise be dependent on this ratio. The results for Nusselt number corresponding to slit and tube flow and $T_{\max}$ for tube flow in terms of De/aL are provided in Table 3. By applying the fractional curve fitting on this set of data, we can find the following correlations:

For slit flow:
$$Nu_r = \frac{0.08428\,De/aL}{0.5544 + De/aL} \tag{28a}$$

For tube flow:
$$Nu_r = \frac{0.1327\,De/aL}{0.5016 + De/aL} \quad \& $$
$$\frac{T_{\max}}{T_{\max,0}} = 1 + \frac{0.03621\,De/aL}{0.4346 + De/aL}. \tag{28b}$$

The above correlations are exact for the Newtonian case and have around 98% confidence for $De/aL \leq 10$. Using the above correlations, Nu and T_{max} can be calculated and these values are necessary to obtain the temperature profiles of FENE-P flow in isothermal slits and tubes.

6 Conclusions

In this article, two exact analytical solutions for heat convection in FENE-P fluid flow through isothermal tubes and slits have been presented for the first time. The closed-form solutions for temperature profiles are obtained based on the modal analysis technique and by considering the scaling law in heat convection. Two fractional correlations for the Nusselt number of slit flow and tube flow are derived in terms of Deborah number and extensibility parameter, key rheological parameters associated with the FENE-P model. It is shown that an increase in the Deborah number and decrease in the extensibility parameter result in an asymptotic increase in the Nusselt number and temperature in the core flow region. It is also found that the Nusselt number and temperature distributions of FENE-P flow are dependent on De/aL. The present method of solution shows significant promise for determining exact solutions for other complicated isothermal systems and fluids described by alternate viscoelastic constitutive equations.

Appendix A: Heun functions

Heun functions are one of the closed form solutions for particular ODEs in mathematics and there are four standard forms, namely *HeunB, HeunC, HeunD and HeunT* which correspond to Biconfluent, Confluent, Doubleconfluent and Triconfluent Heun equations. HeunT function is the solution for the linear differential equation of second order given by:

$$\frac{d^2}{dy^2}f(y) - (3y^2 + \gamma)\frac{d}{dy}f(y) - ((-\beta + 3)y - \alpha)f(y)$$
$$= 0$$

(29)

in which all of the four parameters, $(\alpha, \beta, \gamma, y)$, are algebraic expressions. By solving the Eq. (29) the closed form solution (HeunT) would be derived as follows:

$$f(y) = C_1 HeunT(\alpha, \beta, \gamma, y)$$
$$+ C_2 HeunT(\alpha, -\beta, \gamma, -y)e^{y(y^2+\gamma)}.$$

(30)

Now based on the boundary conditions introduced in Eqs. (31) and (32), the second term in Eq. (30) will vanish, so that Eq. (30) will be simplified to the one given by Eq. (33).

$$at \quad y = 0 \quad \Rightarrow \quad f_{,y} = 0$$

(31)

$$at \quad y = 0 \quad \Rightarrow \quad f = 0$$

(32)

$$f(y) = C_1 HeunT(\alpha, \beta, \gamma, y).$$

(33)

Furthermore, the *HeunT* function could be written in the series solution form. Since the single singularity is located at infinity, this series converges into the entire complex plane. The Handbook of Mathematical functions prepared by the National Institute of Standards and Technology (NIST), Maryland, USA, is an excellent reference for Heun functions.

Appendix B: The Nusselt number and constants of temperature profile

In this section, the polynomial equation of the Nusselt number of FENE-P flow in an isothermal tube has been presented. This polynomial is obtained by applying the boundary condition (14b) to Eq. (24) and considering $C_2 = 0$. According to the scaling law in heat convection, the Nusselt number is the first order root of the following algebraic equation:

$$-\left(\frac{U_N}{U}\right)^7 \left(\begin{array}{c} \frac{1}{3251404800} + \frac{1}{29030400}(\frac{DeU_N}{LUa})^2 + \frac{1}{604800}(\frac{DeU_N}{LUa})^4 + \frac{1}{22680}(\frac{DeU_N}{LUa})^6 \\ + \frac{2}{2835}(\frac{DeU_N}{LUa})^8 + \frac{32}{4725}(\frac{DeU_N}{LUa})^{10} + \frac{512}{14175}(\frac{DeU_N}{LUa})^{12} + \frac{8192}{99225}(\frac{DeU_N}{LUa})^{14} \end{array} \right) Nu^7.$$

$$+ \left(\frac{U_N}{U}\right)^6 \left(\begin{array}{c} -\frac{1}{38707200} - \frac{23}{14515200}(\frac{DeU_N}{LUa})^2 - \frac{1}{36288}(\frac{DeU_N}{LUa})^4 + \frac{1}{5670\,L^6 U^{12} a^6}(\frac{DeU_N}{LUa})^6 + \\ \frac{32}{2835}(\frac{DeU_N}{LUa})^8 + \frac{1856}{14175}(\frac{DeU_N}{LUa})^{10} + \frac{1024}{2025}(\frac{DeU_N}{LUa})^{12} \end{array} \right) Nu^6$$

$$-\left(\frac{U_N}{U}\right)^5 \left(\begin{array}{c} \frac{1}{1382400} + \frac{53}{2419200}(\frac{DeU_N}{LUa})^2 + \frac{13}{453600}(\frac{DeU_N}{LUa})^4 - \frac{1}{378}(\frac{DeU_N}{LUa})^6 \\ + \frac{8}{525}(\frac{DeU_N}{LUa})^8 + \frac{1024}{2835}(\frac{DeU_N}{LUa})^{10} \end{array} \right) Nu^5$$

$$+ \left(\frac{U_N}{U}\right)^4 \left(\frac{4631}{203212800} + \frac{51049}{25401600}(\frac{DeU_N}{LUa})^2 + \frac{28789}{529200}(\frac{DeU_N}{LUa})^4 + \frac{60064}{99225}(\frac{DeU_N}{LUa})^6 + \frac{5056}{2025}(\frac{DeU_N}{LUa})^8 \right) Nu^4$$

$$- \left(\frac{U_N}{U}\right)^3 \left(\frac{59}{51200} + \frac{107003}{1587600}(\frac{DeU_N}{LUa})^2 + \frac{26126}{19845}(\frac{DeU_N}{LUa})^4 + \frac{837248}{99225}(\frac{DeU_N}{LUa})^6 \right) Nu^3$$

$$+ \left(\frac{U_N}{U}\right)^2 \left(\frac{73}{2304} + \frac{551}{450}(\frac{DeU_N}{LUa})^2 + \frac{952}{81}(\frac{DeU_N}{LUa})^4 \right) Nu^2 - \frac{U_N}{U}\left(\frac{3}{8} + \frac{64}{9}(\frac{DeU_N}{LUa})^2 \right) Nu + 1 = 0$$

(34)

The nonzero constant of temperature distribution (C_1) can be determined using the constraint presented in Eq. (15), for $j = 1$, as follows:

$$C_1^{-1} = T_{\max}^{-1} = \frac{4096}{315} Nu^4 \left(\frac{De}{aL}\right)^{10} \left(\frac{U_N}{U}\right)^{15}$$
$$+ \frac{704}{189} Nu^4 \left(\frac{De}{aL}\right)^8 \left(\frac{U_N}{U}\right)^{13} - \frac{1024}{27} Nu^3 \left(\frac{De}{aL}\right)^8 \left(\frac{U_N}{U}\right)^{12}$$
$$+ \frac{80}{189} Nu^4 \left(\frac{De}{aL}\right)^6 \left(\frac{U_N}{U}\right)^{11} - \frac{64}{9} Nu^3 \left(\frac{De}{aL}\right)^6 \left(\frac{U_N}{U}\right)^{10}$$
$$+ \left(\frac{1}{42} \left(\frac{NuDe}{aL}\right)^4 + \frac{18944}{315} Nu^2 \left(\frac{De}{aL}\right)^6\right) \left(\frac{U_N}{U}\right)^9$$
$$- \frac{13}{27} Nu^3 \left(\frac{De}{aL}\right)^4 \left(\frac{U_N}{U}\right)^8 + Nu^2 \left(\frac{1}{1512} \left(\frac{NuDe}{aL}\right)^2\right)$$
$$+ \frac{312}{35} \left(\frac{De}{aL}\right)^4 \left(\frac{U_N}{U}\right)^7 + Nu \left(-\frac{1}{72} \left(\frac{NuDe}{aL}\right)^2\right)$$
$$- \frac{1664}{27} \left(\frac{De}{aL}\right)^4 \left(\frac{U_N}{U}\right)^6$$
$$+ \left(\frac{1}{138240} Nu^4 + \frac{37}{84} \left(\frac{NuDe}{aL}\right)^2\right) \left(\frac{U_N}{U}\right)^5$$
$$+ \left(-\frac{1}{6912} Nu^3 - \frac{272}{45} Nu \left(\frac{De}{aL}\right)^2\right) \left(\frac{U_N}{U}\right)^4$$
$$+ \left(\frac{83}{11520} Nu^2 + \frac{64}{3} \left(\frac{De}{aL}\right)^2\right) \left(\frac{U_N}{U}\right)^3$$
$$- \frac{7}{48} Nu \left(\frac{U_N}{U}\right)^2 + \frac{U_N}{U}.$$

$$(35)$$

References

1. Shah R (1975) Laminar flow friction and forced convection heat transfer in ducts of arbitrary geometry. Int J Heat Mass Transf 18:849–862
2. Shah R, London A (1978) Laminar flow forced convection in ducts. Academic Press, New York
3. Bejan A (1995) Convection heat transfer. 2nd edn. Wiley, New York
4. Kays W, Crawford M (1980) Convective Heat and Mass Transfer. McGraw-Hill, New York
5. Oliveira PJ, Pinho FT (1999) Analytical solution for fully developed channel and pipe flow of Phan-Thien–Tanner fluids. J Fluid Mech 387:271–280
6. Oliveira P (2002) An exact solution for tube and slit flow of a FENE-P fluid. Acta Mech 158:157–167
7. Coelho PM, Pinho FT, Oliveira PJ (2003) Thermal entry flow for a viscoelastic fluid: the Graetz problem for the PTT model. Int J Heat Mass Transf 46:3865–3880
8. Pinho F, Oliveira P (2000) Analysis of forced convection in pipes and channels with the simplified Phan-Thien–Tanner fluid. Int J Heat Mass Transf 43:2273–2287
9. Coelho P, Pinho F, Oliveira P (2002) Fully developed forced convection of the Phan-Thien–Tanner fluid in ducts with a constant wall temperature. Int J Heat Mass Transf 45:1413–1423
10. Filali A, Khezzar L, Siginer D, Nemouchi Z (2012) Graetz problem with non-linear viscoelastic fluids in non-circular tubes. Int J Thermal Sci 61:50–60
11. Shah R, London A (1974) Thermal boundary conditions and some solutions for laminar duct flow forced convection. ASME J Heat Transf 96:159–165
12. Oliveira P, Coelho P, Pinho F (2004) The Graetz problem with viscous dissipation for FENE-P fluids. J Non-Newtonian Fluid Mech 121:69–72
13. Filali A, Khezzar L (2013) Numerical simulation of the Graetz problem in ducts with viscoelastic FENE-P fluids. Comput Fluids 84:1–15
14. Iaccarino G, Shaqfeh ES, Dubief Y (2010) Reynolds-averaged modeling of polymer drag reduction in turbulent flows. J Non-Newtonian Fluid Mech 165:376–384
15. Resende P, Pinho F, Younis B, Kim K, Sureshkumar R (2013) Development of a low-Reynolds-number k-ω Model for FENE-P Fluids. Flow Turbul Combust 90:69–94
16. Resende P, Kim K, Younis B, Sureshkumar R, Pinho F (2011) A FENE-P k–ε turbulence model for low and intermediate regimes of polymer-induced drag reduction. J Non-Newtonian Fluid Mech 166:639–660
17. Khezzar L, Filali A, AlShehhi M (2014) Flow and heat transfer of FENE-P fluids in ducts of various shapes: effect of Newtonian solvent contribution. J Non-Newtonian Fluid Mech 207:7–20
18. Masoudian M, Pinho F, Kim K, Sureshkumar R (2016) A RANS model for heat transfer reduction in viscoelastic turbulent flow. Int J Heat Mass Transf 100:332–346
19. Varagnolo S, Filippi D, Mistura G, Pierno M, Sbragaglia M (2017) Stretching of viscoelastic drops in steady sliding. Soft Matter 13:3116–3124
20. Pinho F, Coelho P (2006) Fully-developed heat transfer in annuli for viscoelastic fluids with viscous dissipation. J Non-Newtonian Fluid Mech 138:7–21
21. Coelho P, Pinho F (2006) Fully-developed heat transfer in annuli with viscous dissipation. Int J Heat Mass Transf 49:3349–3359
22. Jalali A, Hulsen M, Norouzi M, Kayhani M (2013) Numerical simulation of 3D viscoelastic developing flow and heat transfer in a rectangular duct with a nonlinear constitutive equation. Korea Austr Rheol J 25:95–105
23. Siginer DA, Letelier MF (2012) Laminar flow of non-linear viscoelastic fluids in straight tubes of arbitrary contour. Int J Heat Mass Transf 55:2731–2745
24. Siginer DA, Letelier MF (2005) Heat transfer in laminar flow of viscoelastic fluids in straight tubes of arbitrary shape. Annu Trans Nord Rheol Soc 13:137–145
25. Norouzi M, Davoodi M, Bég OA, Joneidi A (2013) Analysis of the effect of normal stress differences on heat transfer in creeping viscoelastic Dean flow. Int J Thermal Sci 69:61–69
26. Zhang M, Shen X, Ma J, Zhang B (2008) Theoretical analysis of convective heat transfer of Oldroyd-B fluids in a curved pipe. Int J Heat Mass Transf 51:661–671

27. Shen X-R, Zhang M-K, Zhang B-Z (2008) Flow and heat transfer of Oldroyd-B fluids in a rotating curved pipe. J Hydrodyn Ser B 20:39–46

28. Norouzi M, Sedaghat M, Shahmardan M (2014) An analytical solution for viscoelastic dean flow in curved pipes with elliptical cross section. J Non-Newtonian Fluid Mech 204:62–71

29. Norouzi M, Biglari N (2013) An analytical solution for Dean flow in curved ducts with rectangular cross section. Phys Fluids 25:053602 **(1994-present)**

30. Hsu CF, Patankar S (1982) Analysis of laminar non-Newtonian flow and heat transfer in curved tubes. AIChE J 28:610–616

31. Norouzi M, Vamerzani BZ, Davoodi M, Biglari N, Shahmardan MM (2015) An exact analytical solution for creeping Dean flow of Bingham plastics through curved rectangular ducts. Rheol Acta 54:391–402

32. Norouzi M, Davoodi M, Anwar Bég O (2015) An analytical solution for convective heat transfer of viscoelastic flows in rotating curved pipes. Int J Thermal Sci 90:90–111

33. Bird R, Dotson P, Johnson N (1980) Polymer solution rheology based on a finitely extensible bead—spring chain model. J Non-Newtonian Fluid Mech 7:213–235

34. Townsend P, Walters K (1994) Expansion flows on non-newtonian liquids. Chem Eng Sci 49:748–763

35. Bird RB, Armstrong R, Hassager O (1987) Dynamics of polymeric liquids. Vol. 1: Fluid mechanics

36. Bird RB, Wiest JM (1995) Constitutive equations for polymeric liquids. Ann Rev Fluid Mech 27:169–193

37. Bird RB (2007) Teaching with FENE dumbbells. Rheol Bull 76:10–12

38. Boyce WE, DiPrima RC (2012) Elementary differential equations and boundary value problems. Wiley, New York

39. Bejan A (2013) Convection heat transfer. Wiley, Hoboken

40. Norouzi M, Davoodi M (2015) Exact analytical solution on convective heat transfer of isothermal pipes. AIAA J Thermophys Heat Transf 29:632–636

41. Canale RP, Chapra SC (2014) Numerical methods for engineers. 7th edn. McGraw-Hill Education, New York

42. Cruz DOA, Pinho FT, Oliveira PJ (2005) Analytical solutions for fully developed laminar flow of some viscoelastic liquids with a Newtonian solvent contribution. J Non-Newtonian Fluid Mech 132:28–35

43. Olver FWJ et al (2010) NIST handbook of mathematical functions. Cambridge University Press, Cambridge